https://doi.org/10.14802/jmd.21178 / J Mov Disord 2022;15(3):232-240
pISSN 2005-940X / eISSN 2093-4939

ORIGINAL ARTICLE

Semiautomated Algorithm for the Diagnosis of Multiple System Atrophy With Predominant Parkinsonism

Woong-Woo Lee,[1,2] Han-Joon Kim,[3,4] Hong Ji Lee,[5] Han Byul Kim,[5] Kwang Suk Park,[5] Chul-Ho Sohn,[6,7] Beomseok Jeon[3,4]

[1]Department of Neurology, Nowon Eulji Medical Center, Eulji University, Seoul, Korea
[2]Department of Neurology, Eulji University College of Medicine, Daejeon, Korea
[3]Department of Neurology, Seoul National University Hospital, Seoul, Korea
[4]Department of Neurology, Seoul National University College of Medicine, Seoul, Korea
[5]Department of Biomedical Engineering, Seoul National University College of Medicine, Seoul, Korea
[6]Department of Radiology, Seoul National University Hospital, Seoul, Korea
[7]Department of Radiology, Seoul National University College of Medicine, Seoul, Korea

ABSTRACT

Objective Putaminal iron deposition is an important feature that helps differentiate multiple system atrophy with predominant parkinsonism (MSA-p) from Parkinson's disease (PD). Most previous studies used visual inspection or quantitative methods with manual manipulation to perform this differentiation. We investigated the value of a new semiautomated diagnostic algorithm using 3T-MR susceptibility-weighted imaging for MSA-p.

Methods This study included 26 MSA-p, 68 PD, and 41 normal control (NC) subjects. The algorithm was developed in 2 steps: 1) determine the image containing the remarkable putaminal margin and 2) calculate the phase-shift values, which reflect the iron concentration. The next step was to identify the best differentiating conditions among several combinations. The highest phase-shift value of each subject was used to assess the most effective diagnostic set.

Results The raw phase-shift values were present along the lateral margin of the putamen in each group. It demonstrates an anterior-to-posterior gradient that was identified most frequently in MSA-p. The average of anterior 5 phase shift values were used for normalization. The highest area under the receiver operating characteristic curve (0.874, 80.8% sensitivity, and 86.7% specificity) of MSA-p versus PD was obtained under the combination of 3 or 4 vertical pixels and one dominant side when the normalization methods were applied. In the subanalysis for the MSA-p patients with a longer disease duration, the performance of the algorithm improved.

Conclusion This algorithm detected the putaminal lateral margin well, provided insight into the iron distribution of the putaminal rim of MSA-p, and demonstrated good performance in differentiating MSA-p from PD.

Keywords Automation; Multiple system atrophy; Parkinson's disease; Putamen; Susceptibility-weighted image.

Multiple system atrophy (MSA) is a rapidly progressive neurodegenerative disease characterized by parkinsonism, cerebellar dysfunction, and dysautonomia.[1,2] The key findings of MSA neuropathology are widespread α-synuclein-positive glial cy-

Received: December 8, 2021 **Revised:** December 29, 2021 **Accepted:** March 10, 2022
Corresponding author: Beomseok Jeon, MD, PhD
Department of Neurology, Seoul National University Hospital, 101 Daehak-ro, Jongno-gu, Seoul 03080, Korea / **Tel:** +82-2-2072-2876 / **Fax:** +82-2-3672-7553/ **E-mail:** brain@snu.ac.kr

toplasmic inclusions and neurodegeneration in the striatonigral or olivopontocerebellar system.[3,4] These pathological features became the essential condition for "definite MSA" in the second consensus criteria for the diagnosis of MSA. However, it is impossible to make a pathological diagnosis of living patients.

The diagnostic criteria of probable MSA and possible MSA are based on clinical features of automatic dysfunction, parkinsonism, and cerebellar dysfunction. However, there are several difficulties associated with providing an early differential diagnosis with these clinical criteria. Autonomic dysfunctions, a core feature of MSA, were not observed at onset in 59% of patients, although they developed in most cases throughout the disease period.[5] In addition, many cases of MSA with predominant parkinsonism (MSA-p) show asymmetric onset (43%) and L-dopa responsiveness (42.5%).[6,7] Thus, early MSA-p can mimic Parkinson's disease (PD).[8,9] This clinical heterogeneity contributes to the low level of diagnostic accuracy.[10,11]

Since Bhattacharya et al.[12] suggested a diagnostic algorithm for MSA, brain magnetic resonance imaging (MRI) has received attention as a promising tool for differential diagnoses. The representative findings of conventional MRI for MSA are reported as follows: 1) atrophy, low signal intensity on T2, and lateral hyperintensity rim sign on T2 for the putamen; 2) atrophy and a "hot-cross bun" sign for the brainstem; and 3) atrophy and high signal intensity of the middle cerebellar peduncle on T2 for the cerebellum. As MRI and nuclear imaging data became more available for MSA, diagnostic imaging findings were newly introduced in the second set of consensus criteria for additional features: 1) atrophy on MRI of the putamen, middle cerebellar peduncle, pons, or cerebellum; and 2) hypometabolism on fluorodeoxyglucose-positron emission tomography in the putamen, brainstem, or cerebellum in possible MSA-p.[2] Recent advances in the instruments themselves and processing techniques have contributed to the increased diagnostic accuracy.[13,14]

Abundant accumulations of iron and putaminal atrophy in MSA-p, although it is unclear which feature appears first, are commonly found in posterolateral areas of the putamen.[15-17] Accordingly, susceptibility-weighted imaging (SWI) and its related techniques, which reflect the degree of iron accumulation,[18] have been developed to achieve early and accurate diagnosis.[19-21] These advanced magnetic resonance (MR) processing techniques improved the sensitivity and specificity for diagnosing MSA-p.[22] However, there are still unsolved issues related to obtaining a higher diagnostic yield. The critical issues are rater-related factors. The selected image cut and region of interest may be inconsistent between raters. Thus, many studies have suggested analyzing interrater reliability. In addition, the issue of intrarater reliability should be considered, especially in the case of visual assessment. Quantification has been suggested as an alternative method of overcoming the issue of inconsistency related to a visual assessment. We also performed a study on the differentiation between MSA-p and PD using the quantification method of the phase-shift value, which reflects the iron contents.[21] However, although the quantified analysis differentiated MSA-p from PD relatively well, it seems to still be arbitrary in determining the region of interest.

Individualization is another important issue. Iron distribution patterns in the normal putamen change depending on age and location.[23] Older age and a more posterolateral location in the putamen are more likely to result in a higher iron concentration. In other words, the iron distribution of the putamen in aged individuals can appear like that in MSA-p patients. Therefore, regardless of the consideration of the individual iron distribution pattern, the fixed cutoff value may not be suitable for the image-based differentiation of MSA-p from the normal population or PD patients. The aims of the current study were to overcome the inconsistency and individualization issues and to enhance the diagnostic accuracy for MSA-p with 3T-MR SWI by adopting a semiautomated algorithm with normalization.

MATERIALS & METHODS

This study was conducted according to the Declaration of Helsinki. The study was performed retrospectively, and the records of the patients were anonymized and deidentified prior to the analysis. Written informed consent for the clinical records was waived because of the guaranteed anonymity and deidentification. The study protocol was approved by the Institutional Review Board of Seoul National University Hospital (IRB#: H-2008-083-1148).

Subjects

The included patients fulfilled the following criteria: 1) visited the Movement Disorder Center of the Seoul National University Hospital due to parkinsonism, 2) underwent 3T brain MRI including SWI from 2010 to 2012, and 3) were clinically diagnosed with either PD or MSA-p (possible, probable) at their last visit (until Dec. 2013) during the follow-up period.[2,24] Even though some patients with MSA-p had cerebellar symptoms, all of them showed parkinsonism as an initial and/or predominant symptom. Forty-one normal control (NC) subjects who had no clinical features of neurodegenerative disorders and underwent brain MRI with the same protocol as that used in the PD and MSA-p groups were also included. Subjects who had white matter changes over Fazekas' grade 1, space-occupying or destructive lesions on brain images, or a history of neurosurgical procedures, including deep brain stimulation before brain

imaging, were excluded from the study. Finally, 135 subjects (26 with MSA-p, 68 with PD, and 41 NCs) were included. Among the 26 cases with MSA-p, 20 were diagnosed with probable MSA-p and 6 with possible MSA-p based on the final diagnosis at the last visit. Other clinical features, such as age at onset, sex, age at the brain MRI visit, and age at the last visit, were obtained from the medical records.

MRI protocol

The subjects underwent 3T brain MRI for SWI with a 32-channel head coil. Magnetom Verio (Siemens, Erlangen, Germany) was used for 3T SWI. All images that were used for the analysis were obtained along the transverse plane parallel to the anterior/posterior commissure lines. The detailed parameters were as follows: for 3T SWI, section thickness = 2 mm, repetition time/echo time = 28.0/20.0 ms, field of view = 178 × 220 mm, matrix = 364 × 448, and number of excitations = 1. Magnitude and phase images were generated for the last SWI on the MR imaging console workstation (syngo MR B17; Siemens, Erlangen, Germany). The corrected phase images were used for the analysis according to the algorithm.

Algorithm to identify the proper target and obtain data

The shapes of the putamen vary from person to person. Thus, we developed an algorithm that consists of Part I and Part II (Figure 1). Part I identifies the axial image that has the most remarkable lateral rim of the putamen. Part II includes the algorithm to detect the margin of both putamina from the selected axial image in Part I, as well as to obtain the calculated phase-shift value data of each point in the margin. The "height" in the algorithm indicates the number of included pixels used to calculate the average value of each point in each axial image. If '3' is input into the "height" box, the algorithm recognizes an average value of 3 sequential pixels in the anterior-to-posterior direction as a newly calculated value of the first point (Supplementary Figure 1 in the online-only Data Supplement).

In Part I, any axial image containing both putamina is selected arbitrarily to start the algorithm. Then, the algorithm automatically moves up and down to search for the appropriate axial image with the most remarkable lateral margin (using edge detection and region-growing methods). If the identified image is rotated, the proper data on the lateral rim may not be obtained. Therefore, as the first step of Part II, the algorithm re-rotated the identified image based on the axis of the falx cerebri. Then, the investigator drew a crude box including the area of interest and marked the first and last points of the lateral rim for each putamen (4 points for each subject) on the selected area. Finally, the algorithm visualized the selected lateral margins of both putamina and obtained the raw data of the calculated phase-shift values at each location. All the above-described steps were performed repeatedly according to the "height" number, which ranged from 1 to 4. One researcher who was blinded to the diagnosis performed all the manual processes. The data that support the conclusions of this study are available from the corresponding author.

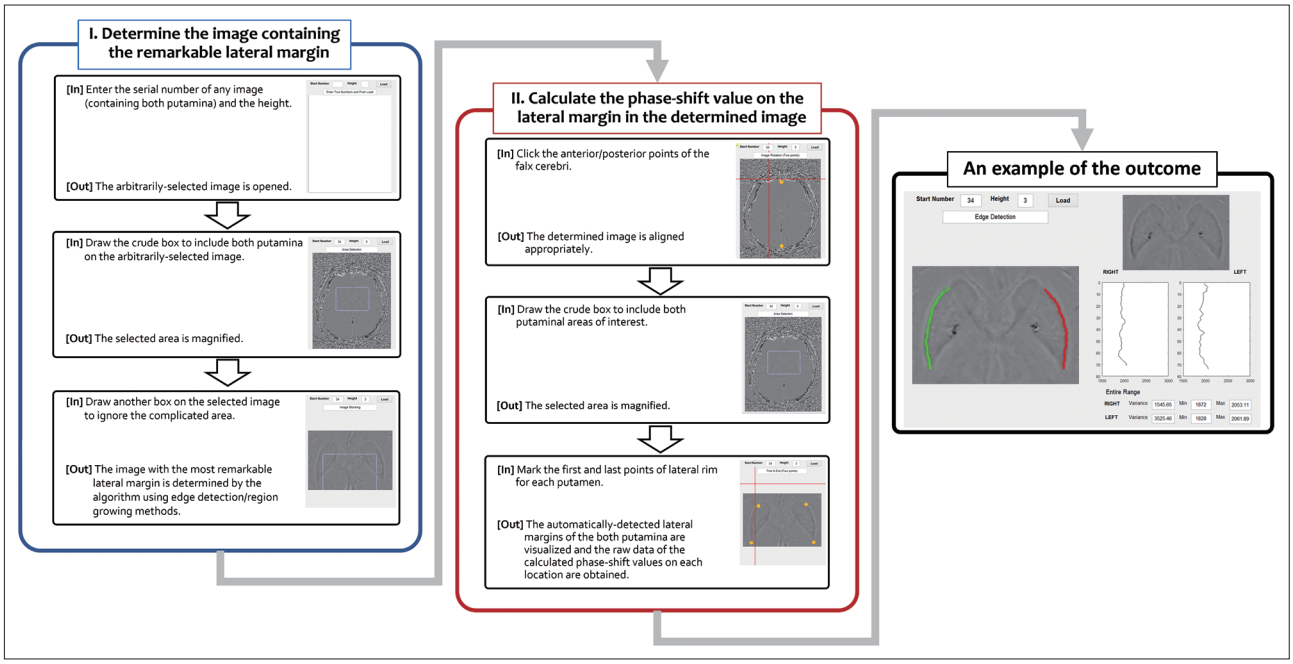

Figure 1. Detailed process of the algorithm. Dark and white signals indicate high and low phase-shift values, respectively.

Statistics

All processes were performed using MATLAB R2015a (MathWorks, Natick, MA, USA) for algorithm development and activation. SPSS software version 21.0 (IBM Co., Armonk, NY, USA) was used for the statistical analysis. Independent *t* tests and ANOVA were performed to assess the differences between the groups as appropriate. The receiver operating characteristic (ROC) curve was analyzed to obtain the most effective combination for the proper diagnosis of MSA-p. The statistical significance level was set at $p < 0.05$.

RESULTS

Clinical characteristics

The clinical characteristics of each group are summarized in Table 1. There were no significant differences with respect to sex and age at onset or at the time of brain MRI. The duration from onset to the time of work-up was significantly shorter in the MSA-p group. The period between onset and the last visit was also shorter for MSA-p patients. Six patients (23.1%) had cerebellar symptoms, and 7 patients (26.9%) exhibited partial levodopa responsiveness in the MSA-p group.

Application of the semiautomated quantitative algorithm

The putaminal lateral margins of all subjects in the MSA-p group were well detected, while those of 8 (11.8%) in the PD group and 2 (4.9%) in the NC group were not discriminated by our algorithm. The possible reasons for the lack of discrimination are as follows: unclear lateral margin for 2 PD patients and vascular lesions with or without diffuse homogenous signal change of the putamen for 6 PD patients and 2 NC subjects.

One hundred twenty-five (92.6%) of the 135 subjects showed well-demarcated margins. We scattered the raw data of each subject in each group (Figure 2). The MSA-p group showed a wide distribution of calculated phase-shift values, while the PD and NC groups tended to consistently exhibit similar values. For the groupwise comparison, we displayed the mean phase-shift values of each section cut into 5 pixels (Figure 3). The posterior parts, especially the 3rd quarter, of the putaminal lateral margin in the MSA-p group exhibited higher values than the anterior sides. The most anterior parts had consistent patterns and similar phase-shift values ($p = 0.517$) regardless of group. This consistency of the anterior parts was expected to be useful in normalizing the individual raw data. Therefore, we adopted the average of anterior 5 phase shift values (AV5) for normalization.

Development of the optimal algorithm for differentiating MSA-p

To enhance the diagnostic accuracy of MSA-p, we experimented with the given phase-shift values under various conditions: 1) by the analyzed side(s) (both sides, one dominant side); 2) by the "height" number (1, 2, 3, 4); and 3) by the normalization methods (raw value, raw value/AV5). In each situation, the highest phase-shift value was defined as the representative raw value. The specific representative raw value for each subject was used for the diagnosis of MSA-p versus PD or NC. The values for the areas under the curve (AUCs) from the ROC curve analysis were calculated for all diagnostic settings (Table 2, Figure 4). All the results were statistically significant ($p < 0.001$).

The AUCs tended to be higher with a larger vertical pixel number after normalization with AV5 and for one dominant side (Table 2, Figure 4). The highest AUC for differentiating MSA-p from PD was 0.874 when the ROC analysis was performed with the representative value obtained from the condition of '3' or '4' vertical pixels, 'raw value/AV5', and 'for one dominant side' (80.8% sensitivity and 86.7% specificity). In this setting, the means ± standard deviations (SDs) of the representative raw values in the MSA-p and PD groups were 2,488.6 ± 356.2 and 2,211.5 ± 52.4 ($p < 0.001$), respectively. The raw values/AV5 were 1.179 ± 0.163 and 1.046 ± 0.022 ($p < 0.001$), respectively.

In the comparison of the MSA-p and NC groups, 0.883 was the highest value in the condition with '3' vertical pixels, 'raw value/AV5', and 'for one dominant side' (80.8% sensitivity and 89.7% specificity). The means ± SDs of the representative raw values in the MSA-p and NC groups were 2,488.6 ± 356.2 and 2,205.6 ± 47.3 ($p < 0.001$), respectively. The raw values/AV5 were 1.179 ± 0.163 and 1.045 ± 0.021 ($p < 0.001$), respectively. All representative values were located on the posterior parts of the putamina.

Table 1. Clinical characteristics of each group

	MSA-p	PD	NC	*p*-value
Number of subjects [male:female]	26 [11:15]	68 [35:33]	41 [16:25]	0.414
Age at brain MRI (yr)	64.4 ± 10.0	64.0 ± 8.2	61.0 ± 10.3	0.189
Age at onset (yr)	61.9 ± 10.6	58.2 ± 10.2	NA	0.124
Duration between onset and brain imaging (yr)	2.5 ± 1.4	5.9 ± 4.9	NA	< 0.001
Duration between onset and last visit (yr)	3.9 ± 1.5	8.2 ± 5.1	NA	< 0.001

Values are presented as mean ± standard deviation unless otherwise indicated. MSA-p, multiple system atrophy with predominant parkinsonism; PD, Parkinson's disease; NC, normal control; MRI, magnetic resonance imaging; NA, not applicable.

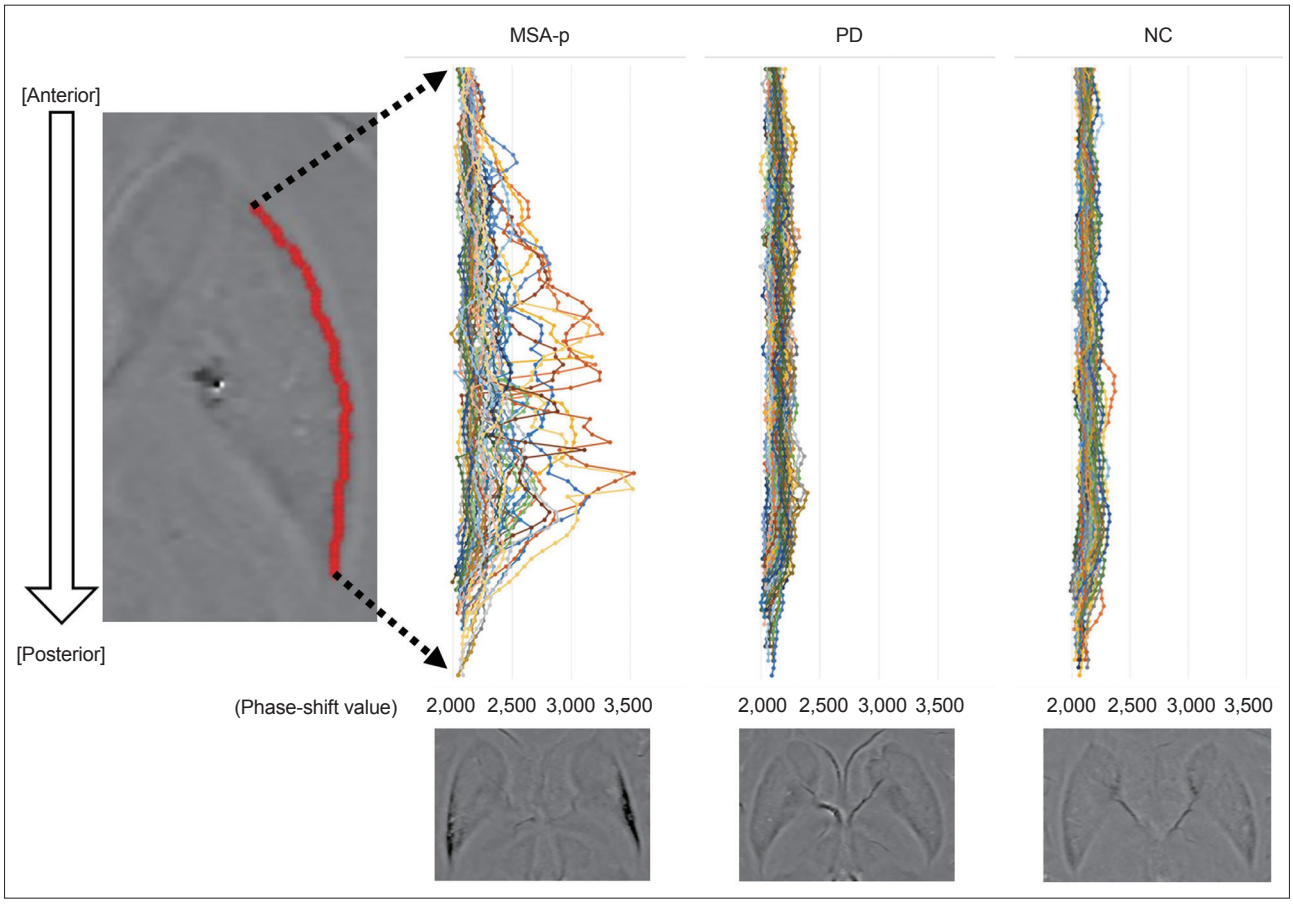

Figure 2. Scatterplot for the phase-shift values of the multiple system atrophy with predominant parkinsonism (MSA-p), Parkinson's disease (PD), and normal control (NC) groups. The figures below show representative examples of each group. Dark and white signals indicate high and low phase-shift values, respectively.

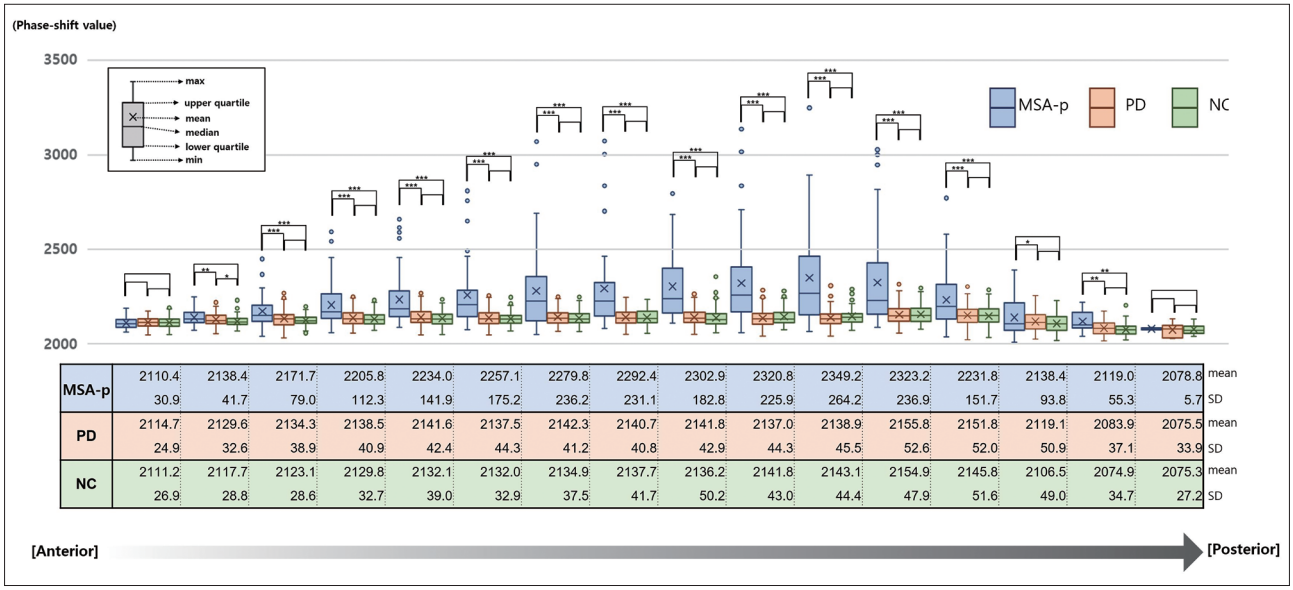

MSA-p	2110.4	2138.4	2171.7	2205.8	2234.0	2257.1	2279.8	2292.4	2302.9	2320.8	2349.2	2323.2	2231.8	2138.4	2119.0	2078.8	mean
	30.9	41.7	79.0	112.3	141.9	175.2	236.2	231.1	182.8	225.9	264.2	236.9	151.7	93.8	55.3	5.7	SD
PD	2114.7	2129.6	2134.3	2138.5	2141.6	2137.5	2142.3	2140.7	2141.8	2137.0	2138.9	2155.8	2151.8	2119.1	2083.9	2075.5	mean
	24.9	32.6	38.9	40.9	42.4	44.3	41.2	40.8	42.9	44.3	45.5	52.6	52.0	50.9	37.1	33.9	SD
NC	2111.2	2117.7	2123.1	2129.8	2132.1	2132.0	2134.9	2137.7	2136.2	2141.8	2143.1	2154.9	2145.8	2106.5	2074.9	2075.3	mean
	26.9	28.8	28.6	32.7	39.0	32.9	37.5	41.7	50.2	43.0	44.4	47.9	51.6	49.0	34.7	27.2	SD

Figure 3. Anterior-to-posterior distribution of the phase-shift values. This figure displays the phase-shift values of each section according to the subgroups. Each section was cut into 5 pixels from the anterior to the posterior parts. All the data in this figure were obtained under the condition of '3' height. *p < 0.05; **p < 0.01; ***p < 0.001. MSA-p, multiple system atrophy with predominant parkinsonism; PD, Parkinson's disease; NC, normal control; SD, standard deviation.

Subgroup analysis of the MSA-p subjects with a longer disease duration

The number of MSA-p subjects with a disease duration of two or more years was 20. We compared them with the PD subjects according to the dominant side. The highest AUC for differentiating MSA-p from PD was 0.893 when we used the condition of '3' vertical pixels and 'raw value/AV5' (Table 3). In the case of the MSA-p subjects with a disease duration of three or more years (n = 13), the highest AUC was 0.906 under the same conditions.

Table 2. Areas under the curve according to the diagnostic set

	For both sides				For one dominant side			
	1	2	3	4	1	2	3	4
MSA-p vs. PD								
Raw value	0.792	0.812	0.811	0.831	0.829	0.838	0.843	0.843
Raw value/AV5	0.812	0.817	0.829	0.845	0.841	0.836	0.874*	0.874*
MSA-p vs. NC								
Raw value	0.818	0.824	0.823	0.837	0.853	0.843	0.847	0.846
Raw value/AV5	0.844	0.813	0.836	0.835	0.873	0.830	0.883*	0.867

All cases reached statistical significance (p < 0.001). The numerals (1 to 4) at first line indicate height. *the most representative cases in each comparison set. MSA-p, multiple system atrophy with predominant parkinsonism; PD, Parkinson's disease; NC, normal control; AV5, the average of anterior 5 phase shift values.

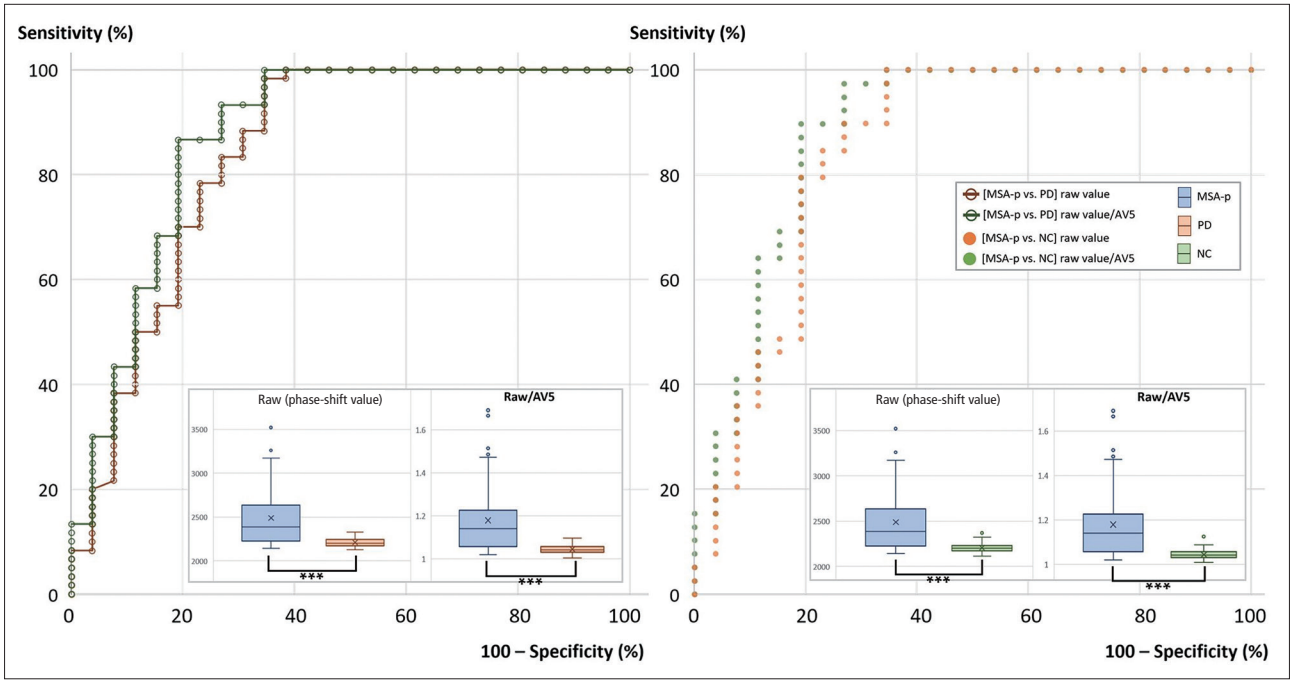

Figure 4. Receiver operating characteristic curves of multiple system atrophy with predominant parkinsonism (MSA-p) versus Parkinson's disease (PD) and MSA-p versus normal control (NC). ***p < 0.001. All the curves represented in this figure were obtained under the condition of 'for one dominant side' and '3' vertical pixels. AV5, the average of anterior 5 phase shift values.

Table 3. Subanalysis for the areas under the curve by the disease duration of MSA-p

	≥ 2 yr (n = 20)				≥ 3 yr (n = 13)			
	1	2	3	4	1	2	3	4
MSA-p vs. PD								
Raw value	0.848	0.865	0.855	0.852	0.851	0.879	0.863	0.855
Raw value/AV5	0.868	0.868	0.893*	0.888	0.881	0.868	0.906*	0.905

All cases reached statistical significance (p < 0.001). The numerals (1 to 4) at first line indicate height. *the most representative cases in each comparison set. MSA-p, multiple system atrophy with predominant parkinsonism; PD, Parkinson's disease; AV5, the average of anterior 5 phase shift values.

DISCUSSION

The early and accurate diagnosis of neurodegenerative disorders is challenging and an important issue in terms of intervening in disease progression. The problem is that early symptoms of MSA-p resemble those of other parkinsonian disorders, and some manifestations arise in the late stage of the disease.[10,14] Many imaging studies have been performed to overcome limitations from a symptom-based diagnosis.[12,25-28] Nevertheless, image-based diagnostics still have limitations results from inconsistent manipulation and interpretation. Thus, we introduced a semiautomated algorithm to solve the problem of inconsistency by human raters.

Additionally, in this newly developed algorithm, we focused on the lateral part of the putamen because previous pathological and imaging studies revealed that the most prominent pathological changes in MSA-p start at the posterolateral rim of the putamen.[16,21,29] The introduced algorithm worked well for all individuals in the MSA-p group. In other words, the putaminal margins of MSA-p were clear enough to be easily detected by the algorithm. Interestingly, it was not successful in some cases in the PD and NC groups. Their margins were unlikely to be demarcated because of homogenous and similar signals compared with those in the surrounding regions.

After applying the algorithm, we identified several important features from the scatterplots of phase-shift values in the putaminal lateral rims. First, the graphs of the PD and NC groups resembled each other. Their variations in the phase-shift values are relatively narrow from the anterior to posterior parts. This lateral margin analysis would be ineffective in differentiating PD from NC. Second, the MSA-p group showed wide intra- and interindividual variations in the phase-shift values. In particular, the highest and most diverse phase-shift values were located on the posterior parts, which is in good agreement with previous reports showing that iron deposition is more predominant in the posterolateral portion of the putamen.[16,21,29] Thus, further imaging studies for the differentiation of MSA-p need to focus more on the posterolateral part of the putamen rather than the whole area. Third, the most interesting result from the scatterplot analysis is that the phase-shift values of the most anterior portion are quite stable in the MSA-p, PD and NC groups. Therefore, we expected that AV5 may reflect an individual iron background in the putamen regardless of the disorder.

AV5 worked well to improve diagnostic accuracy. In the ROC curve analysis, when the normalization method using AV5 was applied, the values of AUCs increased markedly rather than when only 'raw values' were used. There were other factors that were helpful in increasing the AUC values. Several studies reported that many MSA-p patients had asymmetry of parkinsonism with compatible asymmetric putaminal involvement on brain MRI.[6,11,21,30] Therefore, it is presumable that the representative values from one dominant side rather than from both sides could make the differences more distinct. Using a large number of vertical pixels also seemed to enhance accuracy. However, further analysis is required to confirm whether 3 or 4 pixels are the most appropriate or larger numbers have additional benefits.

The diagnostic accuracy in the current study improved compared with that in the previous quantitative study using the phase-shift values.[21] The highest values of AUC, sensitivity, and specificity in this study were 0.874, 80.8%, and 86.7%, respectively, while those in the previous study were 0.803, 77.8%, and 76.0.[21] There are several explanations for the improvement. We utilized all lateral margins and determined the most characteristic values to maximize the differences. We normalized each raw data point with the initial five phase-shift values of each individual subject. In addition, 16 situations were examined for each comparison, and the most effective setting was selected. If the discrimination failure cases by our algorithm were regarded as 'no MSA-p,' the diagnostic yield could increase even more. In the further analysis for the MSA-p patients with a longer disease duration, the AUC values increased up to 0.893 (for the cases of disease duration ≥ two years) and 0.906 (for the cases of disease duration ≥ three years).

There are several limitations of this study. First, this study is not based on definite MSA. There could be MSA-p-mimicking conditions, such as PD with early prominent autonomic dysfunction and levodopa responsiveness. Because it is difficult to perform a study with only definite MSA in practice, this is an unavoidable issue in clinical studies. We followed the patients more from the time of the work-up, and the proportion of probable MSA-p at the final visit was high (20 of 26, 76.9%). Second, data were collected retrospectively from medical records. The data on clinical severity were not included. Additionally, there could be selection bias. Third, there was a discrepancy between the MSA-p and PD groups in the follow-up period and the duration between the onset and the brain MRI visit. It is widely known that MSA-p progresses more rapidly than PD.[5-7] We included more follow-up clinical data even after the acquisition of brain MRI to render the diagnoses more reliable. Additionally, the ages at the workup were not different between the groups. This means that the confounding effects associated with the age factor, which is well correlated with iron accumulation in the putamen, may be negligible.[23] Fourth, there was no direct comparison with visual assessment, and we collected the SWI data generated by one particular type of MRI machine. Additional investigations are required to prove the superiority of the new algorithm and to apply it to other iron-specific imaging modali-

ties. Finally, the current algorithm works semiautomatically. The current algorithm still requires users' help in several steps to prevent detection errors, as shown in Figure 1. It could not be excluded that these manual processes may affect the outcomes of the algorithm. Automating the algorithm to function without the user's intervention and improving all processes from image selection to final diagnosis are currently in progress.

In conclusion, the semiautomated algorithm using the SWI data is helpful in overcoming rater-related problems and enhancing the diagnostic accuracy of MSA-p from PD. Additionally, we suggested a new personalized approach to reflect the individual iron background and the most effective combinations of several conditions to increase the diagnostic yield. If these additional features could be reflected in the advanced algorithm, the diagnostic yield would be better.[19,31] Further studies are necessary beyond the current limitations with the rapid progression of artificial intelligence.

Supplementary Materials

The online-only Data Supplement is available with this article at https://doi.org/10.14802/jmd.21178.

Conflicts of Interest

The authors have no financial conflicts of interest.

Funding Statement

This work was supported by a National Research Foundation of Korea (NRF) grant funded by the Korean government (MSIT) (No. 2017R1C1B5074597).

Author Contributions

Conceptualization: Woong-Woo Lee, Chul-Ho Sohn, Beomseok Jeon. Data curation: Woong-Woo Lee, Hong Ji Lee, Han Byul Kim. Formal analysis: Woong-Woo Lee, Hong Ji Lee, Han Byul Kim. Funding acquisition: Woong-Woo Lee. Investigation: Woong-Woo Lee, Beomseok Jeon. Methodology: Woong-Woo Lee, Beomseok Jeon. Project administration: Woong-Woo Lee, Beomseok Jeon. Resources: Han-Joon Kim, Chul-Ho Sohn, Beomseok Jeon. Software: Hong Ji Lee, Han Byul Kim. Supervision: Han-Joon Kim, Kwang Suk Park, Chul-Ho Sohn. Validation: Woong-Woo Lee. Visualization: Woong-Woo Lee, Hong Ji Lee, Han Byul Kim. Writing—original draft: Woong-Woo Lee. Writing—review & editing: Woong-Woo Lee, Han-Joon Kim, Kwang Suk Park, Chul-Ho Sohn, Beomseok Jeon.

ORCID iDs

Woong-Woo Lee	https://orcid.org/0000-0002-8767-7967
Han-Joon Kim	https://orcid.org/0000-0001-8219-9663
Hong Ji Lee	https://orcid.org/0000-0002-9096-7105
Han Byul Kim	https://orcid.org/0000-0002-7375-9195
Kwang Suk Park	https://orcid.org/0000-0003-1892-6816
Chul-Ho Sohn	https://orcid.org/0000-0003-0039-5746
Beomseok Jeon	https://orcid.org/0000-0003-2491-3544

REFERENCES

1. Gilman S, Low PA, Quinn N, Albanese A, Ben-Shlomo Y, Fowler CJ, et al. Consensus statement on the diagnosis of multiple system atrophy. J Neurol Sci 1999;163:94-98.
2. Gilman S, Wenning GK, Low PA, Brooks DJ, Mathias CJ, Trojanowski JQ, et al. Second consensus statement on the diagnosis of multiple system atrophy. Neurology 2008;71:670-676.
3. Jellinger KA. Neuropathology of multiple system atrophy: new thoughts about pathogenesis. Mov Disord 2014;29:1720-1741.
4. Wenning GK, Tison F, Ben Shlomo Y, Daniel SE, Quinn NP. Multiple system atrophy: a review of 203 pathologically proven cases. Mov Disord 1997;12:133-147.
5. Wenning GK, Ben Shlomo Y, Magalhães M, Daniel SE, Quinn NP. Clinical features and natural history of multiple system atrophy. An analysis of 100 cases. Brain 1994;117(Pt 4):835-845.
6. Low PA, Reich SG, Jankovic J, Shults CW, Stern MB, Novak P, et al. Natural history of multiple system atrophy in the USA: a prospective cohort study. Lancet Neurol 2015;14:710-719.
7. Wenning GK, Geser F, Krismer F, Seppi K, Duerr S, Boesch S, et al. The natural history of multiple system atrophy: a prospective European cohort study. Lancet Neurol 2013;12:264-274.
8. Quinn NP. How to diagnose multiple system atrophy. Mov Disord 2005;20 Suppl 12:S5-S10.
9. Albanese A, Colosimo C, Bentivoglio AR, Fenici R, Melillo G, Colosimo C, et al. Multiple system atrophy presenting as parkinsonism: clinical features and diagnostic criteria. J Neurol Neurosurg Psychiatry 1995;59:144-151.
10. Osaki Y, Ben-Shlomo Y, Lees AJ, Wenning GK, Quinn NP. A validation exercise on the new consensus criteria for multiple system atrophy. Mov Disord 2009;24:2272-2276.
11. Koga S, Aoki N, Uitti RJ, van Gerpen JA, Cheshire WP, Josephs KA, et al. When DLB, PD, and PSP masquerade as MSA: an autopsy study of 134 patients. Neurology 2015;85:404-412.
12. Bhattacharya K, Saadia D, Eisenkraft B, Yahr M, Olanow W, Drayer B, et al. Brain magnetic resonance imaging in multiple-system atrophy and Parkinson disease: a diagnostic algorithm. Arch Neurol 2002;59:835-842.
13. Brooks DJ, Seppi K; Neuroimaging Working Group on MSA. Proposed neuroimaging criteria for the diagnosis of multiple system atrophy. Mov Disord 2009;24:949-964.
14. Stankovic I, Quinn N, Vignatelli L, Antonini A, Berg D, Coon E, et al. A critique of the second consensus criteria for multiple system atrophy. Mov Disord 2019;34:975-984.
15. Kaindlstorfer C, Jellinger KA, Eschlböck S, Stefanova N, Weiss G, Wenning GK. The relevance of iron in the pathogenesis of multiple system atrophy: a viewpoint. J Alzheimers Dis 2018;61:1253-1273.
16. Matsusue E, Fujii S, Kanasaki Y, Sugihara S, Miyata H, Ohama E, et al. Putaminal lesion in multiple system atrophy: postmortem MR-pathological correlations. Neuroradiology 2008;50:559-567.
17. Lee MJ, Kim TH, Kim SJ, Mun CW, Shin JH, Lee GH, et al. Speculating the timing of iron deposition in the putamen in multiple system atrophy. Parkinsonism Relat Disord 2019;63:106-110.
18. Hopp K, Popescu BF, McCrea RP, Harder SL, Robinson CA, Haacke ME, et al. Brain iron detected by SWI high pass filtered phase calibrated with synchrotron X-ray fluorescence. J Magn Reson Imaging 2010;31:1346-1354.
19. Lee JY, Yun JY, Shin CW, Kim HJ, Jeon BS. Putaminal abnormality on 3-T magnetic resonance imaging in early parkinsonism-predominant multiple system atrophy. J Neurol 2010;257:2065-2070.
20. Liu C, Li W, Tong KA, Yeom KW, Kuzminski S. Susceptibility-weighted imaging and quantitative susceptibility mapping in the brain. J Magn Reson Imaging 2015;42:23-41.
21. Hwang I, Sohn CH, Kang KM, Jeon BS, Kim HJ, Choi SH, et al. Differentiation of parkinsonism-predominant multiple system atrophy from idiopathic Parkinson disease using 3T susceptibility-weighted MR imaging, focusing on putaminal change and lesion asymmetry. AJNR Am J Neuroradiol 2015;36:2227-2234.
22. Lee JH, Lee MS. Brain iron accumulation in atypical Parkinsonian syndromes: in vivo MRI evidences for distinctive patterns. Front Neurol 2019;10:74.
23. Li W, Wu B, Batrachenko A, Bancroft-Wu V, Morey RA, Shashi V, et al. Differential developmental trajectories of magnetic susceptibility in hu-

man brain gray and white matter over the lifespan. Hum Brain Mapp 2014; 35:2698-2713.
24. Gelb DJ, Oliver E, Gilman S. Diagnostic criteria for Parkinson disease. Arch Neurol 1999;56:33-39.
25. Massey LA, Micallef C, Paviour DC, O'Sullivan SS, Ling H, Williams DR, et al. Conventional magnetic resonance imaging in confirmed progressive supranuclear palsy and multiple system atrophy. Mov Disord 2012;27:1754-1762.
26. Meyer PT, Frings L, Rücker G, Hellwig S. 18F-FDG PET in parkinsonism: differential diagnosis and evaluation of cognitive impairment. J Nucl Med 2017;58:1888-1898.
27. Orimo S, Suzuki M, Inaba A, Mizusawa H. 123I-MIBG myocardial scintigraphy for differentiating Parkinson's disease from other neurodegenerative parkinsonism: a systematic review and meta-analysis. Parkinsonism Relat Disord 2012;18:494-500.
28. Bajaj S, Krismer F, Palma JA, Wenning GK, Kaufmann H, Poewe W, et al. Diffusion-weighted MRI distinguishes Parkinson disease from the parkinsonian variant of multiple system atrophy: a systematic review and meta-analysis. PLoS One 2017;12:e0189897.
29. Han YH, Lee JH, Kang BM, Mun CW, Baik SK, Shin YI, et al. Topographical differences of brain iron deposition between progressive supranuclear palsy and parkinsonian variant multiple system atrophy. J Neurol Sci 2013;325:29-35.
30. Batla A, Stamelou M, Mensikova K, Kaiserova M, Tuckova L, Kanovsky P, et al. Markedly asymmetric presentation in multiple system atrophy. Parkinsonism Relat Disord 2013;19:901-905.
31. Scherfler C, Göbel G, Müller C, Nocker M, Wenning GK, Schocke M, et al. Diagnostic potential of automated subcortical volume segmentation in atypical parkinsonism. Neurology 2016;86:1242-1249.

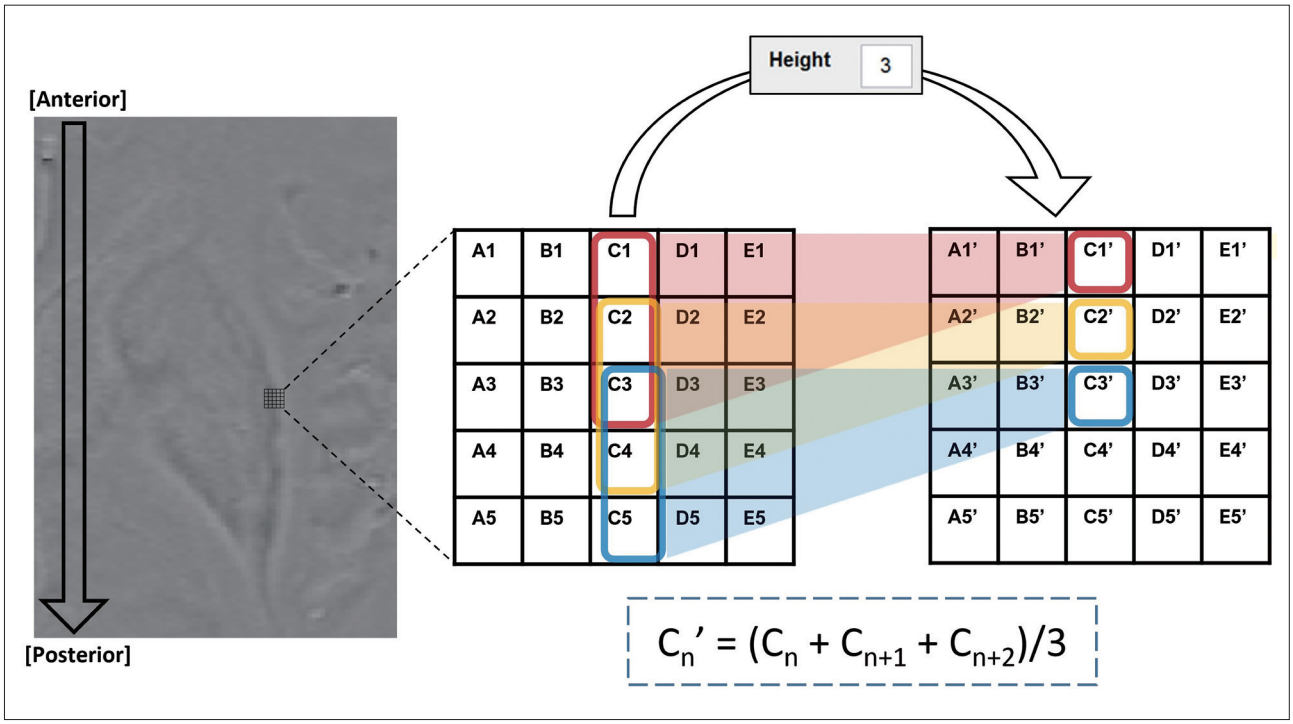

Supplementary Figure 1. Schematic explanation of the 'height.' The 'height' means the number of included pixels used to calculate the average value of each point in each axial image. If '3' is input into the 'height' box, the algorithm recognizes an average value of 3 sequential pixels in the anterior-to-posterior direction as a newly calculated value of the first point.